



m-Terphenylphosphines: Synthesis, structures and coordination properties

Bryan Buster^a, Armando A. Diaz^a, Tillman Graham^a, Rabiya Khan^a, Masood A. Khan^a, Douglas R. Powell^a, Rudolf J. Wehmschulte^{b,*}

^a Department of Chemistry and Biochemistry, University of Oklahoma, 620 Parrington Oval, Room 208, Norman, OK 73019, United States

^b Department of Chemistry, Florida Institute of Technology, 150 W. University Blvd., Melbourne, FL 32901, United States

ARTICLE INFO

Article history:

Received 9 January 2009
Received in revised form 17 March 2009
Accepted 24 March 2009
Available online 31 March 2009

Keywords:

Phosphine
Ruthenium complex
Bulky ligand
X-ray crystal structure
Density functional theory
NMR
Chelate complex
Intramolecular coordination
Arene complex

ABSTRACT

A series of *m*-terphenylphosphines TerphPCl₂, TerphPH₂ and TerphPMe₂ (Terph = 2,6-Mes₂C₆H₃–, 2,6-(4-*t*-BuC₆H₄)₂C₆H₃–, 2,6-(3,5-Me₂C₆H₃)₂C₆H₃–, 2,6-(2,6-Et₂C₆H₃)₂C₆H₃–, and 2,6-(2,6-*i*-Pr₂C₆H₃)₂C₆H₃–; Mes = 2,4,6-Me₃C₆H₂–) was prepared and fully characterized. The structural investigation by X-ray crystallography and density functional theory revealed significant distortions in the environment of the *ipso* carbon and phosphorus centers. These can be traced back to steric interactions and repulsions of the chlorine and methyl substituents on phosphorus with one of the flanking arenes of the *m*-terphenyl substituents. The primary phosphine 2,6-Mes₂C₆H₃PH₂, **6**, and the dimethylphosphine 2,6-(3,5-Me₂C₆H₃)₂C₆H₃PMe₂, **9**, readily form complexes with the Cl₂Ru(*p*-cymene) complex fragment, whereas the larger phosphine 2,6-Mes₂C₆H₃PMe₂, **8**, does not. Heating of the complexes TerphPR₂Ru(Cl₂)(*p*-cymene) **11** and **12** and the mixture of **8** and {(*p*-cymene)RuCl₂}₂ lead to expulsion of the *p*-cymene ligand and intramolecular η⁶ coordination of one of the flanking arene rings to the ruthenium center to afford the complexes Cl₂RuP(H₂)C₆H₃-2-η⁶-Mes-6-Mes, **13**, Cl₂RuP(Me₂)C₆H₃-2-η⁶-Mes-6-Mes, **14**, and Cl₂RuP(H₂)C₆H₃-2-η⁶-(3,5-Me₂C₆H₃)-6-(3,5-Me₂C₆H₃), **15**. All complexes were characterized by NMR spectroscopy and complexes **14** and **15** also by X-ray crystallography.

© 2009 Elsevier B.V. All rights reserved.

1. Introduction

Organophosphorous compounds bearing large substituents have been successfully applied to stabilize unusual oxidation states or coordination environments [1–3]. In recent years, sterically encumbered electron-rich trialkyl- and biphenyldialkylphosphines have been employed as supporting ligands in various catalyzed C–C, C–N or C–O coupling reactions [4,5]. A relatively new class of bulky substituents are *m*-terphenyls [6,7]. During our work on unsymmetrical 9-phosphafluorenes, which were prepared by facile intramolecular C–H activation in *m*-terphenyldichlorophosphines TerphPCl₂ [8,9], we have obtained several X-ray crystal structures of these precursors. Since these compounds featured relatively large distortions of the C–C_{*ipso*}–P angles, we then prepared the related methyl or hydrogen substituted compounds TerphPMe₂ and TerphPH₂ and determined the structures of two of these to better understand the reasons for these distortions. The experimental data have been supported by quantum mechanical calculations. In addition, the coordination properties of selected phosphines TerphPMe₂ and TerphPH₂ were probed by their interactions with

{(*p*-cymene)RuCl₂}₂, and the X-ray crystal structures of two representative complexes were determined.

2. Experimental

2.1. General procedures

All work was performed under anaerobic and anhydrous conditions by using either modified Schlenk techniques or an Innovative Technologies or Vacuum Atmospheres drybox. Solvents were freshly distilled under N₂ from sodium, potassium or sodium/potassium alloy and degassed twice prior to use. *n*-Butyllithium (1.6 M in hexanes), methyllithium (1.5 M in Et₂O), methylmagnesium bromide (2.6 M in THF), and PCl₃ were obtained from commercial suppliers. 2,6-Et₂C₆H₃Br [10], 2,6-(2,6-*i*-Pr₂C₆H₃)₂C₆H₃I [11], 2,6-Mes₂C₆H₃PCl₂, **1** [12,13], 2,6-(4-*t*-BuC₆H₄)₂C₆H₃PCl₂, **2** [14], 2,6-(3,5-Me₂C₆H₃)₂C₆H₃PCl₂, **3** [8], and 2,6-Mes₂C₆H₃PH₂, **6** [12], were synthesised according to literature methods. NMR spectra were recorded on a Varian Mercury 300 MHz, a Varian Unity Plus 400 MHz or a Bruker Avance 400 MHz spectrometer, and ¹H NMR chemical shift values were determined relative to the residual protons in C₆D₆ or CDCl₃ as internal reference (δ = 7.15 or 7.27 ppm). ¹³C NMR spectra were referenced to the solvent signal (δ = 128.0 or 77.0 ppm) and ³¹P NMR spectra were referenced to

* Corresponding author. Tel.: +1 321 674 7659; fax: +1 321 674 8951.
E-mail address: rwehmsch@fit.edu (R.J. Wehmschulte).

Table 1
Crystal data and structural refinement for compounds **1**, **3**, **4**, **6**, **7**, **9**, **10**, **14** and **15**.

	1^c	3	4	6	8	9	10	14	15 · CDCl₃
Empirical formula	C ₂₄ H ₂₅ Cl _{1.91} I _{0.05} P _{0.95}	C ₂₂ H ₂₁ Cl ₂ P	C ₂₆ H ₂₉ Cl ₂ P	C ₂₄ H ₂₇ P	C ₂₆ H ₃₁ P	C ₂₄ H ₂₇ P	C ₅₂ H ₅₈ P ₂	C ₂₆ H ₃₁ Cl ₂ PRu	C ₂₅ H ₂₈ Cl ₅ PRu
Formula weight	416.44	387.26	443.36	346.43	374.48	346.43	744.92	546.45	637.76
T (K)	98(2)	98(2)	98(2)	173(2)	120(2)	100(2)	173(2)	293(2)	99(2)
Wavelength (Å)	0.71073	0.71073	0.71073	0.71073	0.71073	0.71073	0.71073	0.71073	0.71073
Crystal system	triclinic	monoclinic	monoclinic	orthorhombic	orthorhombic	monoclinic	monoclinic	monoclinic	monoclinic
Space group	P $\bar{1}$	P2(1)/c	P2(1)/n	Cmc2(1)	P2(1)2(1)2(1)	P2(1)/c	P2(1)/c	Pc	P2(1)/n
a (Å)	8.824(2)	10.2237(6)	7.5113(3)	23.20(2)	7.7542(8)	10.3378(4)	11.213(4)	19.122(7)	8.9261(10)
b (Å)	8.939(2)	23.8919(13)	14.6869(7)	13.165(11)	14.7337(14)	24.3603(10)	16.355(4)	8.207(3)	27.417(3)
c (Å)	15.867(4)	8.2733(5)	20.6494(9)	6.567(5)	19.0484(19)	8.1965(3)	23.544(7)	15.917(6)	10.8952(12)
α (°)	77.595(6)	90	90	90	90	90	90	90	90
β (°)	76.772(6)	104.4120(10)	92.5510(10)	90	90	104.4470(10)	94.32(3)	96.929(9) ^o	103.636(2)
γ (°)	61.812(5)	90	90	90	90	90	90	90	90
V (Å ³)	1065.5(4)	1957.3(2)	2275.74(17)	2006(3)	2176.2(4)	1998.87(13)	4305(2)	2479.7(16)	2591.2(5)
Z	2	4	4	4	4	4	4	4	4
D _{calc} (mg/m ³)	1.298	1.314	1.294	1.147	1.143	1.151	1.149	1.464	1.635
μ (Mo K α) (mm ⁻¹)	0.437	0.415	0.366	0.140	0.134	0.141	0.135	0.923	1.196
F(0 0 0)	436	808	936	744	808	744	1600	1120	1288
Crystal size (mm ³)	0.32 × 0.24 × 0.18	0.28 × 0.26 × 0.20	0.46 × 0.36 × 0.22	0.48 × 0.28 × 0.12	0.36 × 0.24 × 0.22	0.38 × 0.24 × 0.12	0.42 × 0.38 × 0.32	0.24 × 0.20 × 0.12	0.26 × 0.18 × 0.16
Crystal color and habit	colorless prism	colorless prism	colorless plate	colorless plate	colorless prism	colorless plate	orange prism	red prism	red rod
2 θ _{max} (°)	26.00	27.49	27.50	25.02	27.50	27.50	24.01	28.33	27.50
Number of observations	6063	4451	5205	1410	4982	4575	6722	11751	5924
Number of variables	255	230	266	125	252	232	495	558	295
R ₁ ^a [I > 2 σ (I)]	0.0328	0.0411	0.0384	0.0500	0.0355	0.0370	0.0817	0.0181	0.0215
wR ₂ ^b [I > 2 σ (I)]	0.0973	0.1154	0.0954	0.1280	0.0968	0.1043	0.1826	0.0499	0.0545
Goodness-of-fit on F ²	1.004	1.009	1.034	1.037	1.047	1.036	1.015	1.028	1.113
Largest difference of peak (e Å ⁻³)	0.366	0.553	1.281	0.177	0.546	0.389	0.737	0.573	0.525

^a $R_1 = \sum ||F_o| - |F_c|| / \sum |F_o|$.

^b $wR_2 = (\sum w||F_o| - |F_c||^2 / \sum w|F_o|^2)^{1/2}$.

^c Contains 5% 2,6-Mes₂C₆H₃l.

external 85% H₃PO₄. Mass spectra were recorded with a JEOL Accu-TOF direct analysis in real time (DART) spectrometer or on a Micro-mass Q-ToF (ESI) spectrometer. UV/vis spectra for compound **10** were collected with an Agilent 8453 spectrophotometer. Melting points were determined in Pyrex capillary tubes (sealed under nitrogen) with a Mel-Temp apparatus and are uncorrected.

2.2. 2,6-(2,6-Et₂C₆H₃)₂C₆H₃I

This compound was prepared in analogy to the literature [15,16] starting with 2,6-Et₂C₆H₃I, and it was purified by crystallization from ethanol. Yield: 47%. M.p. 102–103 °C. ¹H NMR (400 MHz, C₆D₆): 7.26 (t, *J* = 7.6 Hz, *p*'-H, 2H), 7.12 (d, *J* = 7.6 Hz, *m*'-H, 4H), 7.03 (t, *J* = 7.6 Hz, *p*-H, 1H), 6.8 (d, *J* = 7.6 Hz, *m*-H, 2H), 2.47 (dq, *J* = 14.8 Hz, 7.4 Hz, CH₂, 4H), 2.38 (dq, *J* = 14.8 Hz, 7.4 Hz, CH₂, 4H), 1.12 (t, CH₃, 12H), 7.4 Hz. ¹³C{¹H} NMR (100.57 MHz, C₆D₆): 146.97, 144.11, 141.42, 128.77, 128.51, 127.90, 126.04 (*m*'-C), 109.69 (*C*-I), 27.03 (CH₂), 15.10 (CH₃).

2.3. 2,6-(2,6-Et₂C₆H₃)₂C₆H₃PCl₂, **4**

A solution of 2,6-(2,6-Et₂C₆H₃)₂C₆H₃I (3.81 g, 8.1 mmol) in hexanes (60 mL) was treated with *n*-BuLi (1.6 M in hexanes, 5.45 mL, 8.7 mmol) at 0 °C, whereupon the color changed to yellow. The reaction mixture was warmed to room temperature and stirred overnight. The volatile material was distilled from the yellow suspension. The remaining pale yellow solid was suspended in hexanes (50 mL), cooled to –78 °C, and freshly distilled PCl₃ (0.76 mL, 8.7 mmol) was added via syringe. The mixture was slowly warmed to room temperature and stirred for another 10 h. The precipitated colorless solid was collected on a sintered glass frit, dissolved in toluene (40 mL) and filtered. The resulting pale yellow solution was concentrated under reduced pressure to ca. 5 mL and cooled to –30 °C for 2 days to give a pale yellow

microcrystalline solid (1.11 g). Concentration of the mother liquor and subsequent cooling to –30 °C for 1 week gave a second batch of small crystals (0.25 g). Yield: 1.36 g, 38%. M.p. 128–131 °C. ¹H NMR (300 MHz, C₆D₆): δ 7.24 (t, *J* = 7.8 Hz, *p*-H(Dep), 2H), 7.07 (d, *J* = 7.8 Hz, *m*-H(Dep), 4H), 7.04 (t, *J* = 7.5 Hz, *p*-H, 1H), 6.90 (dd, *J* = 7.5 Hz, *J*_{HP} = 3.0 Hz, *m*-H, 2H), 2.49 (dq, *J* = 15 Hz, 7.5 Hz, CH₂, 4H), 2.36 (dq, *J* = 15 Hz, 7.5 Hz, CH₂, 4H), 1.06 (t, 7.5 Hz, CH₃, 12H). ¹³C{¹H} NMR (75.45 MHz, C₆D₆): δ 146.29 (d, *J*_{CP} = 28.9 Hz), 142.63 (d, *J*_{CP} = 2.6 Hz, *o*-C(Dep)), 137.55 (d, *J*_{CP} = 8.3 Hz), 134.65 (d, *J*_{CP} = 73.0 Hz, *i*-C), 131.85 (*p*-C), 131.19 (d, *J*_{CP} = 1.1 Hz, *m*-C), 129.02 (*p*-C(Dep)), 125.64 (*m*-C(Dep)), 28.02 (CH₂CH₃), 15.22 (CH₂CH₃). ³¹P{¹H} NMR (121.47 MHz, C₆D₆): δ 160.2. MS (DART): *m/z* 443.133 (M+H⁺). Anal. Calc. for C₂₆H₃₀Cl₂P⁺: 443.146.

2.4. 2,6-(2,6-*i*-Pr₂C₆H₃)₂C₆H₃PCl₂, **5**

A solution of *n*-BuLi (1.6 M in hexanes, 5 mL, 8.0 mmol) was added to a solution of 2,6-(2,6-*i*-Pr₂C₆H₃)₂C₆H₃I (3.80 g, 7.2 mmol) in hexanes (50 mL) at 0 °C. After about 1 h a fine colorless precipitate began to form. The mixture was slowly warmed to room temperature and stirred for an additional 2 h. The precipitate was collected on a sintered glass frit and dried in vacuo to give 2.34 g of product which was identified as almost pure 2,6-(2,6-*i*-Pr₂C₆H₃)₂C₆H₃Li by ¹H NMR spectroscopy. A small amount of benzene insoluble material was assumed to be LiI. A suspension of this solid in hexanes (40 mL) was added dropwise (20 min) to a solution of freshly distilled PCl₃ in hexanes at –78 °C. The mixture was kept at that temperature for 30 min and then allowed to slowly warm to room temperature. During warm-up the suspension changed color to orange. After stirring at room temperature overnight the mixture was filtered, and the volatile material was removed from the filtrate in vacuo. The resulting pale yellow viscous oil solidified after 2 h at room temperature. It was identified as a 3:1 mixture of 2,6-(2,6-*i*-Pr₂C₆H₃)₂C₆H₃PCl₂ and

Table 2

Experimental and calculated (in parentheses) bond distances (Å) and angles (°) for the *m*-terphenylphosphines TerphPX₂ **1–9**.

	1 ^a X = Cl	2 ^b X = Cl	3 X = Cl	4 X = Cl	5 X = Cl	6 X = H	7 X = H	8 X = Me	9 X = H
P–C _{Terph}	1.847(3) (1.863)	1.837(2) (1.859)	1.8591(17) (1.858)	1.8451(15) (1.864)	(1.864)	1.816(5) (1.860)	(1.867)	1.8602(13) (1.881)	1.8662(11) (1.884)
P–X	2.0556(10) (2.114)	2.0612(9) (2.108)	2.0583(6) (2.108)	2.0592(5) (2.114)	(2.104)	1.33(6) (1.418)	(1.420)	1.8500(13) (1.864)	1.8499(13) (1.875)
	2.0666(11) (2.115)	2.0723(9) (2.131)	2.0785(7) (2.138)	2.0695(5) (2.116)	(2.122)	1.33(6) (1.418)	(1.420)	1.885(2) (1.869)	1.8530(12) (1.875)
X–P–X	98.77(5) (101.3)	100.11(4) (101.5)	99.24(3) (101.4)	100.04(2) (101.1)	(100.7)	116(6) (94.8)	(94.7)	98.23(8) (97.5)	94.37(6) (94.7)
X–P–C _{Terph}	105.53(9) (104.0)	104.53(7) (104.5)	104.46(5) (104.5)	103.35(5) (103.6)	(105.6)	100(3) (98.4)	(97.0)	109.87(6) (109.4)	105.61(5) (103)
	101.28(9) (102.9)	101.93(7) (102.7)	102.08(6) (102.9)	102.64(5) (103.5)	(101.5)	100(3) (98.3)	(97.0)	99.49(8) (102.3)	103.10(5) (102.4)
C _{ortho} –C _{ipso} –P	130.2(2) (129.7)	128.2(2) (128.3)	127.92(13) (128.5)	128.83(11) (129.4)	(130.5)	120.5(2) (120.3)	(120.4)	128.44(10) (128.1)	123.09(8) (121.4)
	109.87(19) (110.6)	111.4(2) (111.2)	111.39(12) (111.1)	111.41(10) (111.0)	(109.9)	120.5(2) (120)	(120.3)	113.24(10) (113.9)	119.80(8) (120.9)
C _{ortho} –C _{ipso} –C _{ortho}	119.9(2) (119.7)	118.9(2) (119.4)	117.08(9) (119.4)	119.74(13) (119.6)	(119.6)	118.9(4) (119.5)	(119.2)	118.31(12) (117.8)	117.08(9) (117.7)
∑(angles at C _{ipso})	359.97 (360.0)	358.5 (358.9)	356.39 (359.0)	359.98 (360)	(360)	359.9 (359.8)	(359.9)	359.99 (359.8)	359.97 (360)
X...H		2.800 (2.820)	2.859 (2.810)						
		2.957 (3.101)	2.984 (3.077)						
Dihedral angle C _{meta} –C _{ortho} –C _{ipso} –P	178.4 (176.8)	163.7 (162.3)	160.4 (162.5)	177.6 (176.6)	(179.2)	178.7 (176.1)	(175.5)	175.2 (176.2)	177.4 (171.2)
	178.1 (177.0)	166.3 (164.6)	163.2 (164.9)	179.3 (177.2)	(179.5)	178.7 (176.1)	(175.5)	175.0 (177.3)	176.8 (171.1)

^a X-ray data from Ref. [13].

^b X-ray data from Ref. [14].

2,6-(2,6-*i*-Pr₂C₆H₃)₂C₆H₃I. Pure product was obtained after recrystallization from hexanes (15 mL) at $-20\text{ }^{\circ}\text{C}$ in form of large (2–3 mm) pale yellow crystals. Yield: 1.15 g, 32% based on 2,6-(2,6-*i*-Pr₂C₆H₃)₂C₆H₃I. M.p. $172\text{--}3\text{ }^{\circ}\text{C}$. ¹H NMR (400.13 MHz, C₆D₆): δ 7.30 (t, $J = 7.7\text{ Hz}$, *p*-H(Dipp), 2H), 7.15 (d, $J = 7.7\text{ Hz}$, *m*-H(Dipp), 4H), 7.07 (m, *p*- and *m*-H, 3H), 2.76 (sept, $J = 6.8\text{ Hz}$, CH(CH₃)₂, 4H), 1.29 (d, $J = 6.8\text{ Hz}$, CH(CH₃)₂, 12H), 1.00 (d, $J = 6.8\text{ Hz}$, CH(CH₃)₂, 12H). ¹³C{¹H} NMR (100.61 MHz, C₆D₆): δ 147.26 (d, $J_{\text{PC}} = 2.2\text{ Hz}$, *o*-C(Dipp)), 145.69 (d, $J_{\text{PC}} = 28.7\text{ Hz}$), 136.50 (d, $J_{\text{PC}} = 8.4\text{ Hz}$), 136.05 (d, $J_{\text{PC}} = 72.6\text{ Hz}$, *i*-C), 132.04 (*p*-C(Dipp) or *m*-C), 130.85 (*p*-C), 129.47 (*p*-C(Dipp) or *m*-C), 123.06 (*m*-C(Dipp)), 31.52 (CH(CH₃)₂), 25.69 (CH(CH₃)₂), 22.78 (CH(CH₃)₂). ³¹P{¹H} NMR (145.78 MHz, C₆D₆): δ 157.6. MS (DART): m/z 499.184 (M+H⁺). Anal. Calc. for C₃₀H₃₈Cl₂P⁺: 499.208.

2.5. 2,6-(4-*t*-BuC₆H₄)₂C₆H₃PH₂, **7**

A solution of **2** (1.81 g, 4.1 mmol) in Et₂O (50 mL) was added slowly to a suspension of LiAlH₄ (0.40 g, 10.5 mmol) in Et₂O at $0\text{ }^{\circ}\text{C}$. The mixture was allowed to warm to room temperature and was stirred overnight. After filtration of the resulting cloudy reaction mixture through a medium porosity glass frit the solvent was distilled off the clear colorless filtrate under reduced pressure, and the remaining colorless solid was extracted with hexanes (60 mL). Concentration to 10 mL and cooling at $-28\text{ }^{\circ}\text{C}$ overnight afforded **7** as thin colorless needles (0.79 g). A second crop (0.21 g) was obtained after concentration to 3 mL and cooling to $-28\text{ }^{\circ}\text{C}$ for 2 days. Yield: 65%. M.p. $125\text{--}127\text{ }^{\circ}\text{C}$. ¹H NMR (400 MHz, C₆D₆): 7.43 (d, $J = 8.2\text{ Hz}$, *o*- or *m*-H (4-*t*-BuC₆H₄), 4H): 7.31 (d, $J = 8.2\text{ Hz}$, *o*- or *m*-H (4-*t*-BuC₆H₄), 4H), 7.23 (dd, $J = 7.2\text{ Hz}$, $J_{\text{HP}} = 2.2\text{ Hz}$, *m*-H, 2H), 7.13 (t, $J = 7.2\text{ Hz}$, *p*-H, 1H), 3.69 (d, $J_{\text{HP}} = 211.2\text{ Hz}$, *p*-H, 2H), 1.23 (s, *p*-C(CH₃)₃). ¹³C{¹H} NMR (100.57 MHz, C₆D₆): 150.38, 147.41 (d, $J_{\text{PC}} = 8.3\text{ Hz}$), 140.81, 129.39 (d, $J_{\text{PC}} = 14.1\text{ Hz}$), 129.04, 127.46, 125.70, 34.57 (C(CH₃)₃), 31.44 (CH₃). ³¹P NMR (161.90 MHz, C₆D₆): -132.0 (t, $J_{\text{PH}} = 211\text{ Hz}$).

2.6. 2,6-Mes₂C₆H₃PMe₂, **8**

A solution of MeMgBr in Et₂O (2.8 mL, 8.4 mmol, 3.0 M) was added dropwise to a solution of **1** in hexanes (70 mL) at $-78\text{ }^{\circ}\text{C}$. The reaction mixture was slowly warmed to room temperature and stirred overnight. Filtration, concentration to 25–30 mL under reduced pressure and crystallization at $-28\text{ }^{\circ}\text{C}$ for 3 d afforded colorless crystals suitable for X-ray diffraction (0.69 g). A second crop was obtained from the concentrated mother liquor (0.31 g). Yield: 1.00 g, 78%. M.p. $147\text{--}149\text{ }^{\circ}\text{C}$. ¹H NMR (300 MHz, C₆D₆): 7.12 (t, $J = 7.5\text{ Hz}$, *p*-H, 1H), 6.84 (s, *m*-H(Mes), 4H), 6.84 (dd, $J = 7.5\text{ Hz}$, $J_{\text{HP}} = 1.8\text{ Hz}$, *m*-H, 2H), 2.20 (s, *p*-Me, 6H), 2.15 (s, *o*-Me, 12H), 0.78 (d, $J = 4.8\text{ Hz}$, PMe, 6H). ¹³C{¹H} NMR (100.57 MHz, C₆D₆): 146.15 (d, $J_{\text{CP}} = 13.7\text{ Hz}$), 139.91, 136.76, 136.12 (*o*-C(Mes)), 129.86 (d, $J_{\text{CP}} = 2.3\text{ Hz}$, *m*-C), 128.79 (*p*-C), 128.46 (*m*-C(Mes)), 21.34 (d, $J_{\text{CP}} = 3.0\text{ Hz}$, *o*-Me), 21.16 (*p*-Me), 13.6 (d, $J_{\text{CP}} = 20.7\text{ Hz}$, PMe). ³¹P{¹H} NMR (121.47 MHz, C₆D₆): -36.4 . MS(FAB): m/z 391.1 (M+O+H⁺, 37%), 375.1 (M+H⁺, 44%), 374.1 (M⁺, 14.2%), 359.1 (M⁺–Me, 100%).

2.7. 2,6-(3,5-Me₂C₆H₃)₂C₆H₃PMe₂, **9**

A solution of **3** (0.92 g, 2.4 mmol) in hexanes (45 mL) was treated with MeMgBr (2.6 M solution in THF, 1.8 mL, 4.7 mmol) at $-78\text{ }^{\circ}\text{C}$. The mixture was warmed to room temperature and stirred overnight. The resulting colorless cloudy reaction mixture was filtered through a medium porosity glass frit, and the solvent was removed under reduced pressure. Recrystallization of the colorless solid from hexanes (20 mL) at $-40\text{ }^{\circ}\text{C}$ for 2 days afforded colorless crystals of **9**. Yield: 0.55 g, 68%. M.p. $96\text{--}98\text{ }^{\circ}\text{C}$. ¹H NMR (300 MHz,

C₆D₆): 7.25 (s, *o*-H(Xyl), 4H), 7.22 (dd (A part of A₂BX system), $J = 8.1\text{ Hz}$, $J_{\text{HP}} = 1.8\text{ Hz}$, 2H), 7.12 (B part of A₂BX system), $J = 8.1\text{ Hz}$, 1H, 6.81 (s, *p*-H(Xyl), 2H), 2.18 (s, *m*-CH₃, 12H), 0.79 (d, $J_{\text{HP}} = 5.4\text{ Hz}$, *p*-CH₃, 6H). ¹³C{¹H} NMR (75.45 MHz, C₆D₆): 148.1, 144.32, 137.71, 129.91, 128.96, 127.96, 127.03, 21.56 (*m*-CH₃), 16.53 (d, $J_{\text{CP}} = 15.8\text{ Hz}$, *p*-CH₃). ³¹P{¹H} NMR (121.47 MHz, C₆D₆): -32.7 . MS(ESI) in CH₃CN solution: m/z 347.2 (M+H⁺).

2.8. [2,6-(2,6-Et₂C₆H₃)₂C₆H₃P]₂, **10**

A solution of **4** (1.00 g, 2.2 mmol) in THF (20 mL) was added to Mg turnings (0.11 g, 4.5 mmol), which had been activated by stirring in THF (20) in the presence of one small crystal of naphthalene. After stirring the mixture at room temperature for 14 h a color change to pale orange was observed. As the color deepened to dark red/purple after two more hours the mixture was filtered through a medium porosity glass frit to give a clear orange solution. The solvent was removed under reduced pressure and the residue was extracted with hexanes (60 mL). The insoluble material was allowed to settle, and the orange supernatant liquid was decanted. Concentration to 2–3 mL and cooling at $-30\text{ }^{\circ}\text{C}$ for 5 d afforded large orange plates of **10**. Yield: 0.21 g, 25%. M.p. color intensified to bright red around $140\text{ }^{\circ}\text{C}$, did not melt below $260\text{ }^{\circ}\text{C}$. ¹H NMR (300 MHz, C₆D₆): 7.19 (t, $J = 7.5\text{ Hz}$, *p*-H(Dipp), 4H), 7.00 (t, $J = 8.1\text{ Hz}$, *p*-H, 2H), 7.00 (t, $J = 7.5\text{ Hz}$, *m*-H(Dipp), 8H), 6.89 (d, $J = 8.1\text{ Hz}$, *m*-H, 4H), 2.17 (m, CH₂, 18H), 1.013 (t, CH₃, 24H). ¹³C{¹H} NMR (75.45 MHz, C₆D₆): 143.66 (d, $J_{\text{CP}} = 16.4\text{ Hz}$), 143.66 (s), 141.69 (*o*-C(Dipp)), 140.82, 129.51, 128.65, 125.56 (*m*-C(Dipp)), 27.18 (CH₂), 14.85 (CH₃). ³¹P{¹H} NMR (121.47 MHz, C₆D₆): 500.6. UV/Vis (hexanes): ϵ (259 nm (sh)) = $11\,070\text{ cm}^{-1}\text{ M}^{-1}$; ϵ (372 nm) = $7920\text{ cm}^{-1}\text{ M}^{-1}$; ϵ (478 nm) = $440\text{ cm}^{-1}\text{ M}^{-1}$.

2.9. (2,6-Mes₂C₆H₃PH₂)RuCl₂(*p*-cymene), **11**

A Schlenk flask was charged with **6** (0.34 g, 1.0 mmol), {(*p*-cymene)RuCl₂)}₂ (0.28 g, 0.45 mmol) and toluene (5 mL). The reaction mixture was stirred overnight to afford a red solution with a fine red-orange solid suspended in it. The solid was dissolved by a brief heating with a heat gun, and the resulting deep red-orange solution was left standing for 7 h at room temperature during which time red-orange crystals formed. Overnight storage at $-20\text{ }^{\circ}\text{C}$ gave some additional crystals. Yield: 0.53 g, 85%. M.p. slight gas evolution at $160\text{ }^{\circ}\text{C}$, melts at $186\text{--}188\text{ }^{\circ}\text{C}$. ¹H NMR (400.13 MHz, CDCl₃): δ 7.52 (td, $J = 7.6\text{ Hz}$, $J_{\text{HP}} = 1.2\text{ Hz}$, *p*-H, 1H), 7.09 (dd, $J = 7.6\text{ Hz}$, $J_{\text{HP}} = 2.9\text{ Hz}$, *m*-H, 2H), 7.00 (s, *m*-H(Mes), 4H), 5.46 (d, $J_{\text{HP}} = 368.2\text{ Hz}$, PH), 4.70 (d, AB system, $J = 5.8\text{ Hz}$, *m*-H(cy), 2H), 4.67 (d, AB system, $J = 5.8\text{ Hz}$, *o*-H(cy), 2H), 2.49 (sept, $J = 6.9\text{ Hz}$, CH(CH₃)₂(cy), 1H), 2.34 (s, *p*-CH₃, 6H), 2.14 (s, *o*-CH₃, 12H), 2.00 (s, *p*-CH₃(cy), 3H), 1.06 (d, $J = 6.9\text{ Hz}$, CH(CH₃)₂(cy), 6H). ¹³C{¹H} NMR (100.62 MHz, CDCl₃): δ 146.86 (d, $J_{\text{PC}} = 8.3\text{ Hz}$, *o*-C), 137.99 (*p*-C(Mes)), 137.86 (d, $J_{\text{PC}} = 4.3\text{ Hz}$, *i*-C(Mes)), 131.10 (*p*-C), 129.92 (d, $J_{\text{PC}} = 7.1\text{ Hz}$, *m*-C), 128.95 (*m*-C(Mes)), 123.45 (d, $J_{\text{PC}} = 47.1\text{ Hz}$, *i*-C), 107.67 (*i*-C(cy)), 103.89 (*p*-C(cy)), 86.01 (d, $J_{\text{PC}} = 4.0\text{ Hz}$, *m*-C(cy)), 84.66 (*o*-C(cy)), 30.31 (CH(CH₃)₂(cy)), 22.28 (CH(CH₃)₂(cy)), 21.52 (*o*-CH₃), 21.32 (*p*-CH₃), 18.11 (*p*-CH₃(cy)). ³¹P NMR (161.97 MHz, CDCl₃): δ -58.2 (t, $J_{\text{HP}} = 368.2\text{ Hz}$).

2.10. (2,6-(3,5-Me₂C₆H₃)₂C₆H₃PMe₂)RuCl₂(*p*-cymene), **12**

A solution of **9** (0.19 g, 0.55 mmol) in benzene (10 mL) was added to {(*p*-cymene)RuCl₂)}₂ (0.17 g, 0.28 mmol), and the suspension was stirred for 1 h at room temperature. The orange microcrystalline solid was isolated. Yield: 0.26 g, 72%. M.p. $340\text{--}350\text{ }^{\circ}\text{C}$ (dec). ¹H NMR (300.07 MHz, CDCl₃): δ 7.33 (td, $J = 7.5\text{ Hz}$, $J_{\text{HP}} = 2.3\text{ Hz}$, *p*-H, 1H), 7.20 (dd, $J = 7.6\text{ Hz}$, $J_{\text{HP}} = 2.4\text{ Hz}$, *m*-H, 2H),

7.07 (s, broad, $w_{1/2} = 8.3$ Hz, *o*-H, 4H), 7.01 (s, *p*-H(3,5-Me₂C₆H₃), 2H), 5.24 (d, *o*- or *m*-H(cy), $J = 5.4$ Hz, 2H), 4.99 (d, *o*- or *m*-H(cy), $J = 5.4$ Hz, 2H), 2.69 (sept, $J = 6.9$ Hz, CH(CH₃)₂(cy), 1H), 2.39 (s, *m*-CH₃, 12H), 1.94 (s, *p*-CH₃(cy), 3H), 1.21 (d, $J_{HP} = 10.8$ Hz, P(CH₃)₂, 6H), 1.07 (d, $J = 6.9$ Hz, CH(CH₃)₂(cy), 6H). ¹³C{¹H} NMR (75.45 MHz, CDCl₃): δ 147.39 (d, $J_{CP} = 11.0$ Hz), 142.16 (d, $J_{CP} = 2.4$ Hz), 136.74, 131.73 (d, $J_{CP} = 7.7$ Hz), 129.28, 128.20, 127.99 (d, $J_{CP} = 3.6$ Hz), 105.55, 95.87, 88.22 (d, $J_{CP} = 4.9$ Hz, *o*- or *m*-C(cy)), 84.69 (d, $J_{CP} = 4.8$ Hz, *o*- or *m*-C(cy)), 30.29 (CH(CH₃)₂), 22.10 (CH(CH₃)₂), 21.52 (*m*-CH₃), 19.50 (d, $J_{CP} = 30.3$ Hz, P(CH₃)₂), 18.45 (CH₃(cy)). ³¹P{¹H} NMR (121.47 MHz, CDCl₃): δ 13.7.

2.11. Cl₂RuP(H₂)C₆H₃-2- η^6 -Mes-6-Mes, **13**

A suspension of **11** (0.24 g, 0.37 mmol) in benzene (10 mL) was dissolved at 75 °C and kept at this temperature for 46 h. After cooling to room temperature the red-orange solid that had precipitated was isolated, washed with benzene (2 × 3 mL) and dried in vacuo to afford the product as an orange mat of very fine needles. Yield: 0.09 g, 47%. M.p. > 260 °C. ¹H NMR (400.13 MHz, CDCl₃): δ 7.80 (t, $J = 7.5$ Hz, *p*-H, 1H), 7.56 (d, $J = 7.6$ Hz, *m*-H, 1H), 7.43 (d, $J = 7.2$ Hz, *m*-H, 1H), 6.99 (s, *m*-H(Mes), 2H), 5.73 (s, *m*-H(η^6 -Mes), 2H), 5.10 (d, $J = 383$ Hz, H-P, 2H), 2.55 (d, $J_{HP} = 4.5$ Hz, *p*-CH₃(η^6 -Mes), 3H), 2.34 (s, *p*-CH₃(Mes), 3H), 1.95 (s, *o*-CH₃(Mes), 6H), 1.79 (s, *o*-CH₃(η^6 -Mes), 6H). ¹³C{¹H} NMR (100.62 MHz, CDCl₃): δ 148.96, 144.55 (d, $J_{PC} = 24.6$ Hz), 138.98, 135.41, 134.95, 134.91, 134.88, 133.74 (d, $J_{PC} = 2.0$ Hz, *p*-C), 130.49 (d, $J_{PC} = 5.5$ Hz, *m*-C), 129.19 (*m*-C(Mes)), 127.14 (d, $J_{PC} = 14.1$ Hz, *m*-C), 104.90 (d, $J_{PC} = 0.4$ Hz, (η^6 -Mes)), 103.69 (d, $J_{PC} = 15.4$ Hz, (η^6 -Mes)), 98.85 (d, $J_{PC} = 4.1$ Hz, *m*-C(η^6 -Mes)), 91.46 (η^6 -Mes), 21.29 (*p*-CH₃(Mes)), 20.64 (*o*-CH₃(Mes)), 17.82 (d, $J_{PC} = 1.5$ Hz, *p*-CH₃(η^6 -Mes)), 17.09 (*o*-CH₃(η^6 -Mes)). ³¹P{¹H} NMR (161.97 MHz, CDCl₃): δ -19.0.

2.12. Cl₂RuP(Me₂)C₆H₃-2- η^6 -Mes-6-Mes, **14**

D-8 toluene (1 mL) was added to a mixture of **8** (8 mg, 0.02 mmol) and {(*p*-cymene)RuCl₂)}₂ (6 mg, 0.01 mmol) in an NMR tube equipped with a Teflon resealable cap. The mixture was heated at 117 °C for 24 h during which time a deep red solution formed. Cooling to room temperature afforded a red-orange microcrystalline solid of **14**. Recrystallization from CDCl₃ and hexane (vapor infusion) gave X-ray quality crystals. ¹H NMR (300.07 MHz, CDCl₃): δ 7.69 (td, $J = 7.5$ Hz, $J_{HP} = 2.0$ Hz, *p*-H, 1H), 7.51 (d, $J = 7.5$ Hz, *m*-H, 1H), 7.23 (ddd, $J = 7.5$ Hz, $J = 1.2$ Hz, $H_{HP} = 1.2$ Hz), 7.01 (s, *m*-H(Mes), 2H), 5.63 (s, *m*-H(η^6 -Mes), 2H), 2.54 (d, $J_{HP} = 4.2$ Hz, *p*-CH₃(η^6 -Mes), 3H), 2.38 (s, *p*-CH₃(Mes), 3H), 1.98 (s, *o*-CH₃(Mes), 6H), 1.75 (s, *o*-CH₃(Mes), 6H), 1.39 (d, $J_{HP} = 12.0$ Hz, P(CH₃)₂, 6H). ¹³C{¹H} NMR (75.45 MHz, CDCl₃): δ 147.43, 144.20 (d, $J_{CP} = 18.3$ Hz), 141.42 (d, $J_{CP} = 31.5$ Hz), 138.79, 133.31, 135.81, 132.57 (d, $J_{CP} = 4.0$ Hz), 132.30, 128.71, 127.23 (d, $J_{CP} = 10.3$ Hz), 104.25, 102.20 (d, $J_{CP} = 10.9$ Hz), 99.37 (d, $J_{CP} = 2.3$ Hz), 88.66, 21.45, 21.40, 17.89, 17.11, 12.35 (d, $J_{CP} = 22.9$ Hz, P(CH₃)₂). ³¹P{¹H} NMR (121.47 MHz, C₆D₆): 44.6.

2.13. Cl₂RuP(Me₂)C₆H₃-2- η^6 -(3,5-Me₂C₆H₃)-6-(3,5-Me₂C₆H₃), **15**

A suspension of **12** (0.03 g, 0.046 mmol) in C₆D₆ (2 mL) in an NMR tube was heated at 95–100 °C for 2.5 h. Upon cooling to room temperature a dark orange solid precipitated. Isolation and recrystallization from CDCl₃/petroleum ether gave X-ray quality crystals of **15**. ¹H NMR (300.07 MHz, CDCl₃): δ 7.55 (m, *m*-H, 2H), 7.37 (m, *p*-H, 1H), 7.15 (s, *p*-H(3,5-Me₂C₆H₃), 1H), 6.99 (s, *o*-H(3,5-Me₂C₆H₃), 2H), 5.94 (s, *p*-H(η^6 -3,5-Me₂C₆H₃), 1H), 4.59 (s, *p*-H(η^6 -3,5-Me₂C₆H₃), 2H), 2.43 (s, *m*-CH₃, 6H), 2.24 (s, *m*-CH₃, 6H), 1.62 (d, $J_{HP} = 12.3$ Hz, P(CH₃)₂, 6H). ¹³C{¹H} NMR (125.69 MHz, CDCl₃): δ 147.56, 139.75, 137.83, 132.41 (d, $J_{CP} = 5.8$ Hz), 130.40,

130.34, 127.82, 126.92 (d, $J_{CP} = 13.8$ Hz), 111.95 (d, $J_{CP} = 2.9$ Hz), 91.94 (d, $J_{CP} = 15.2$ Hz), 21.58 (*m*-CH₃), 19.07 (*m*-CH₃), 17.30 (d, $J_{CP} = 32.3$ Hz, P(CH₃)₂). ³¹P{¹H} NMR (121.47 MHz, C₆D₆): 46.6. MS(ESI) in CH₃CN solution: m/z 541.01 M+Na⁺, 483.05 M-Cl⁻; correct isotope pattern.

2.14. X-ray crystallography

Crystals were removed from the Schlenk tube under a stream of N₂-gas and immediately covered with a layer of hydrocarbon oil. A suitable crystal was selected, attached to a glass fiber, and immediately placed in the low-temperature nitrogen stream. The data for **6** and **10** were collected at 173(2) K on a Siemens P4 diffractometer and those for **1**, **3**, **4**, at 98(2), for **8** at 120(2), for **9** at 100(2), for **14** at 293(2), and for **15** at 99(2) K on a Bruker Apex diffractometer using Mo K α ($\lambda = 0.71073$ Å) radiation. The data were corrected for Lorentz and polarization effects. Absorption corrections based on a multi-scan method from equivalent reflections were used for **1**, **3**, **4**, **8**, **9**, **14**, and **15**. The structures were solved by direct methods using the SHELXTL program suite, Version 5.1 [17] for **6** and **10**, Version 6.12 for **3**, **4**, **8**, **9**, **14**, and **15** and Version 6.14 for **1** and refined by full-matrix least-squares on F^2 including all reflections. Unless stated otherwise, all the non-hydrogen atoms were refined anisotropically and all the hydrogen atoms were included in the refinement with idealized parameters. The crystal of **1** exhibited non-merohedral twinning by a rotation of 180° around the direction (0 0 1) with a twin ratio refined to 0.4989(7). The crystal structure as refined with 100%-PCl₂ contained a large peak in the difference map that was about 2.1 Å from Cl. This peak was believed to be due to a small component of iodine in place of the PCl₂ group, i.e. starting material. The occupancies of the hetero atoms refined to 0.9546(8) for PCl₂ and 0.0454(8) for I. Restraints on the displacement parameters of the disordered atoms were required. Considering the disorder and twinning problems with the structure of **1** the data discussed in the narrative are taken from Ref. [13]. The hydrogen atom bound to P in **6** (H1) was located in the difference map and refined isotropically. The structure of **14** contains two independent molecules, whose metric parameters are very similar. The data discussed here are those of molecule 1 (Ru1). Some details of the crystal data and refinement are given in Table 1, and selected bond distances and angles are listed in Table 2. Further details can be obtained from the Cambridge Crystallographic database under deposition numbers 715808–715816.

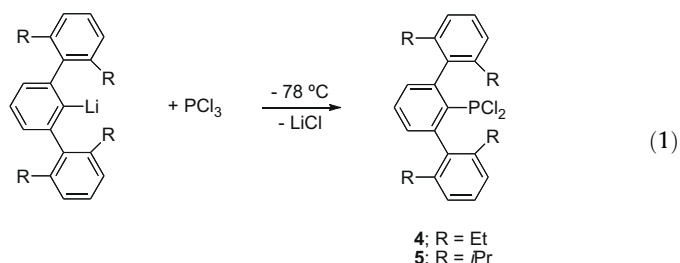
2.15. Computational methods

The geometries for the compounds **1–9** were fully optimized using B3LYP Density Functional Theory with the 6-31G* basis set. Vibrational frequencies were computed for each compound to confirm the absence of imaginary frequencies. Important geometric data are summarized in Table 2. Figures comparing experimental and calculated structures as well as a list of Cartesian coordinates of the calculated structures are provided in the Supporting Information. All computations were performed with the Spartan'04 Macintosh software.

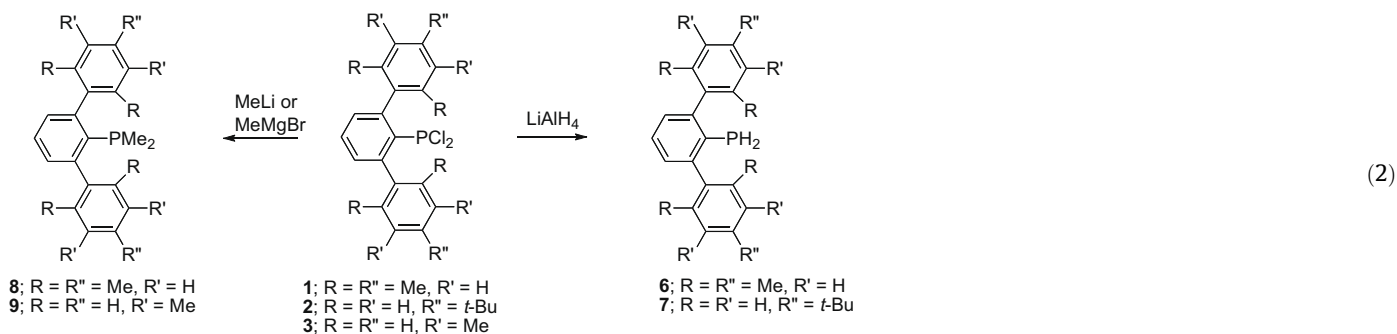
3. Results and discussion

3.1. *m*-Terphenylphosphines

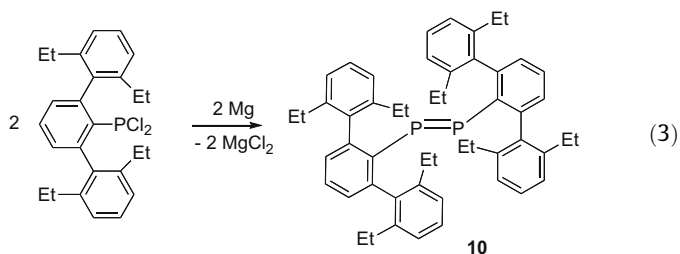
The new *m*-terphenyldichlorophosphines 2,6-(2,6-Et₂C₆H₃)₂-C₆H₃PCl₂, **4**, and 2,6-(2,6-*i*-Pr₂C₆H₃)₂-C₆H₃PCl₂, **5**, were prepared in analogy to the known compounds 2,6-Mes₂C₆H₃PCl₂, **1** [12,13], 2,6-(4-*t*-BuC₆H₄)₂-C₆H₃PCl₂, **2** [14], and 2,6-(3,5-Me₂C₆H₃)₂-C₆H₃-PCl₂, **3** [8], (Eq. (1)) in good to moderate yields.



They have been obtained as colorless to pale yellow moisture sensitive crystals. The presence of lithium iodide in the *m*-terphenyl lithium reagent should be avoided, because it leads to unwanted side reactions. For example, compounds **2** and **3** are partially converted to 9-iodo-9-phosphafluorenes, and *m*-terphenyl iodide is produced during the preparation of **1** and **5** if lithium iodide is present. Reduction of **1** and **2** with LiAlH₄ cleanly afforded the primary phosphines 2,6-Mes₂C₆H₃PH₂, **6** and 2,6-(4-*t*-BuC₆H₄)₂C₆H₃PH₂, **7** in form of moderately air sensitive, colorless crystals. Methylation of **1** and **3** with LiMe or MeMgBr gave access to the colorless, crystalline *m*-terphenyldimethylphosphines 2,6-Mes₂C₆H₃PMe₂, **8** and 2,6-(3,5-Me₂C₆H₃)₂C₆H₃PMe₂, **9** (Eq. (2)).



Compounds **6** [12] and **8** [18] have been reported previously and had been prepared by slightly different methods than those described here. All compounds are readily soluble in standard organic solvents. The solution NMR spectra are simple and reflect the symmetry of these compounds. Long-range ⁴J_{PH} couplings involving the *m*-hydrogens of the central ring with values of 2–3 Hz are observed for most of the compounds. The ³¹P NMR chemical shifts are typical for each class of compounds with ca. 160 ppm for TerphPCl₂ **1–5**, ca. –132 ppm for TerphPH₂ **6** and **7** and ca. –35 ppm for TerphPMe₂ **8** and **9** [19]. Reduction of **4** with magnesium in THF afforded the diphosphene 2,6-(2,6-Et₂C₆H₃)₂C₆H₃P=P=C₆H₃(C₆H₃-Et₂-2,6)₂, **10** as an orange crystalline solid (Eq. (3)) (Figs. 1–6).



3.2. Structures of *m*-terphenylphosphines

Single crystal X-ray structures were obtained for compounds **1–4**, **6**, **8**, and **10**. The structures of **1** [13] and **8** [18] have been reported independently during the time this project has taken place,

and they correspond closely to the structures obtained and discussed here. In addition, energy minimized structures of **1–9** were determined using DFT calculations. In all cases the calculated structures mirror closely the experimental structures lending credence to the calculated structures of **5**, **7**, and **9** for which no experimental data were obtained (Table 2). With the exception of **6** and **9** all *m*-terphenylphosphines display a pronounced distortion at the *ipso* carbon. The phosphorus center is bent towards one of the flanking arene rings of the *m*-terphenyl substituent resulting in C_{ortho}–C_{ipso}–P angles ranging from 109.9° (**1**) to 111.4° (**2–4**) for the narrow angle and 127.9° (**3**) to 130.2° (**1**) for the wide angle. This kind of asymmetry has been previously described for terphenylarsines, stibines and bismuthines [20] and was attributed to the so-called Menshutkin interaction [21]. Whereas the latter interaction can be traced back to an attraction between an electron rich aromatic system and a Lewis acidic arsenic, antimony and bismuth center, the data collected in this study suggest that the here observed distortions are most likely due to steric influences. There are no distortions for the primary phosphines **6** and **7** and only little distortion for the dimethylphosphine **9**. In these compounds the plane bisecting the X–P–X angles is almost orthogonal to the plane

of the central arene ring. Use of the larger 2,6-Mes₂C₆H₃–, 2,6-(2,6-Et₂C₆H₃)₂C₆H₃– and 2,6-(2,6-*i*-Pr₂C₆H₃)₂C₆H₃– substituents in combination with methyl (**8**) and chlorine substituents (**1**, **4** and **5**) leads to the above mentioned significant distortions. Here, the plane bisecting the X–P–X angles is almost parallel with the plane of the central arene ring, and the phosphorus center is leaning towards one of the flanking rings. The combination of the smaller *m*-terphenyl substituents 2,6-(4-*t*-BuC₆H₄)₂C₆H₃– and 2,6-(3,5-Me₂C₆H₃)₂C₆H₃– with chlorine substituents (**2** and **3**) also resulted in large distortions. This is most likely due to secondary H···Cl contacts stabilizing the “parallel” rotamer (as in **1**) as opposed the “orthogonal” rotamer (see **9**). The other geometrical parameters are within their normal range. A reviewer suggested that electronic contributions to the distortions could be manifested in an increase in the pyramidalization of the *ipso* carbon caused by negative

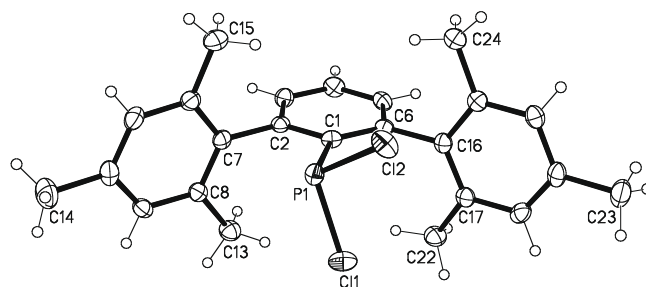


Fig. 1. Molecular structure of **1** (50% ellipsoids).

hyperconjugation between the *ipso* carbon and P–X σ^* -orbitals. However, a significant deviation from planarity as expressed by the sum of the angles at the *ipso* carbon atoms was observed only for compounds **2** ($\sum(\text{angles}) = 358.5^\circ$) and **3** ($\sum(\text{angles}) = 356.4^\circ$) (see Table 2). The $C_{\text{meta}}-C_{\text{ortho}}-C_{\text{ipso}}-P$ dihedral angles mirror this

trend: For compounds **1**, **4**, **6**, and **9** they range from 175.2° to 179.3° , but are much smaller for compounds **2** (163.7° and 166.3°) and **3** (160.4° and 163.2°). Considering that these distortions are practically independent of the nature of the P–X substituent (X = H, Me, and Cl) and the previously stated observation that

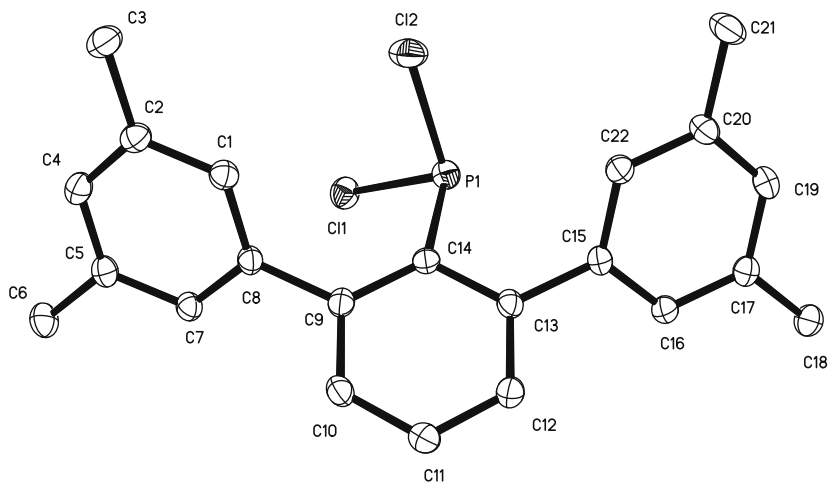


Fig. 2. Molecular structure of **3** (50% ellipsoids). Hydrogen atoms have been omitted for clarity.

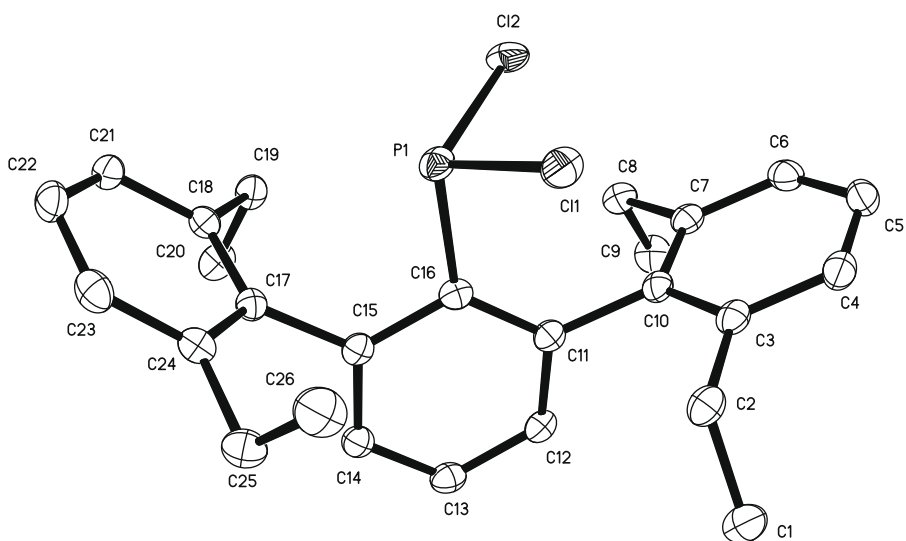


Fig. 3. Molecular structure of **4** (50% ellipsoids). Hydrogen atoms have been omitted for clarity.

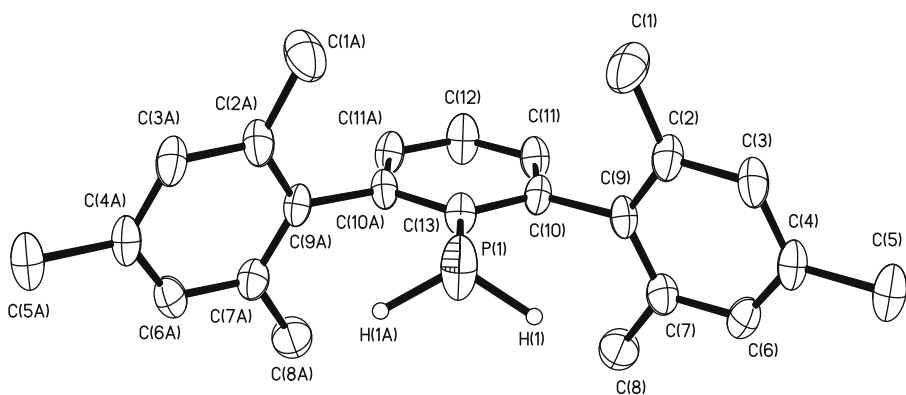


Fig. 4. Molecular structure of **6** (50% ellipsoids). Hydrogen atoms except of those bound to phosphorus have been omitted for clarity.

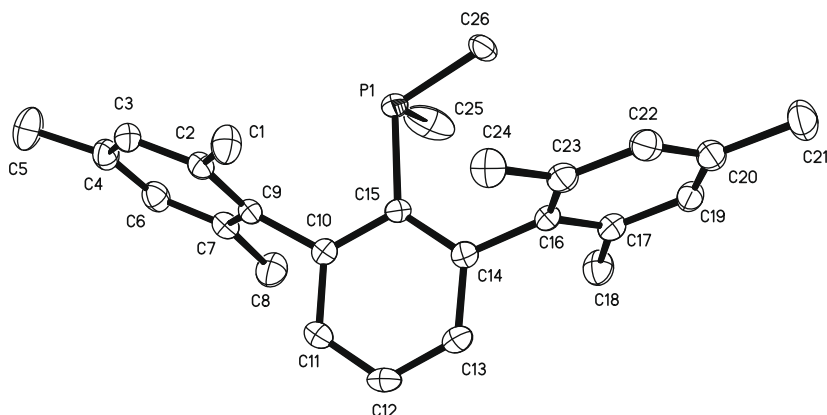


Fig. 5. Molecular structure of **8** (50% ellipsoids). Hydrogen atoms have been omitted for clarity.

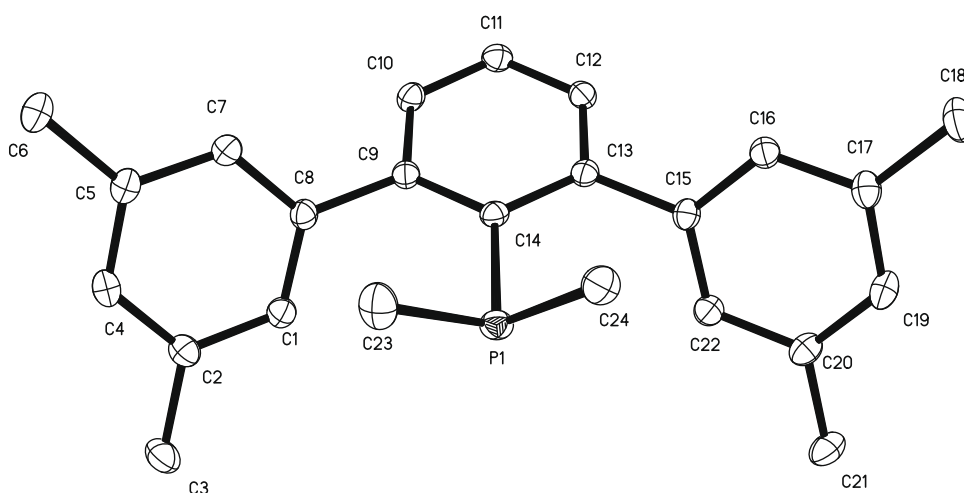


Fig. 6. Molecular structure of **9** (50% ellipsoids). Hydrogen atoms have been omitted for clarity.

large deviations of the $C_{ortho}-C_{ipso}-P$ angles correlate well with the sizes of the *m*-terphenyl and P–X substituents, the observed distortions are most likely due to unfavorable steric interactions. The more pronounced distortions in **2** and **3** can be traced back to secondary H···Cl contacts between the *ortho*-hydrogen atoms of the flanking aromatic rings and one of the two chlorine substituents.

The structure of diphosphene **10** (Fig. 7) is very close to the ones reported for the related $\{2,6\text{-Mes}_2\text{C}_6\text{H}_3\text{P}\}_2$ [12] and $2,6\text{-Mes}_2\text{C}_6\text{H}_3\text{P}=\text{P}-\text{Ar}-\text{P}=\text{PC}_6\text{H}_3\text{-Mes}_2\text{-}2,6$ (Ar = 2,3,5,6-(4-*t*-BuC₆H₄)₄C₆ [22]). The P–P bond distance in **10** with a value of 2.017(2) Å is slightly longer than in the latter ones with values of 1.985(2) and 2.008(2) Å, respectively, but still within the typical range reported for diphosphenes [1]. Furthermore, the orientation of the substituents is such that the central ring of one substituent is approximately coplanar with the C–P=P–C core, and the other one is close to orthogonal to that core (angle between plane normals = 7.4° and 66.5°).

3.3. Ruthenium complexes

The reaction of **6** and **9** with $\{(p\text{-cymene})\text{RuCl}(\mu\text{-Cl})_2\}_2$ at room temperature afforded the complexes $(2,6\text{-Mes}_2\text{C}_6\text{H}_3\text{PH}_2)\text{RuCl}_2(p\text{-cymene})$, **11**, and $(2,6\text{-}(3,5\text{-Me}_2\text{C}_6\text{H}_3)_2\text{C}_6\text{H}_3\text{PMe}_2)\text{RuCl}_2(p\text{-cymene})$, **12**, in good yields as red-orange air-stable solids in analogy to literature reports [23]. Interestingly, the corresponding reaction of

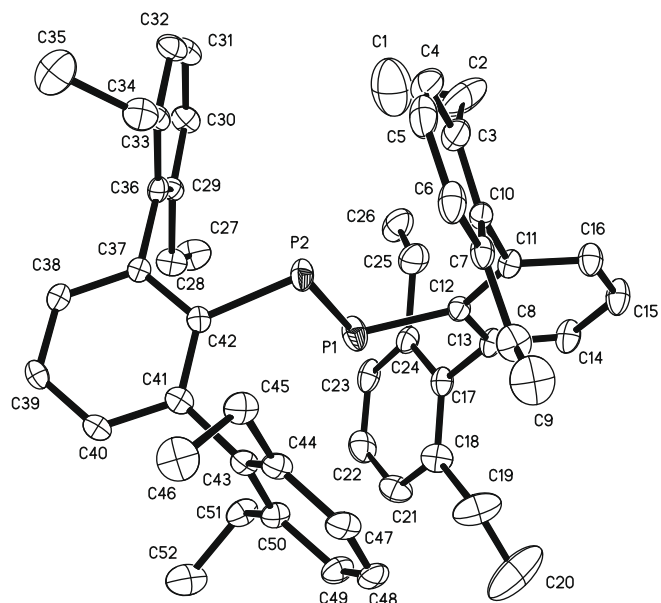


Fig. 7. Molecular structure of **10** (50% ellipsoids). Hydrogen atoms have been omitted for clarity.

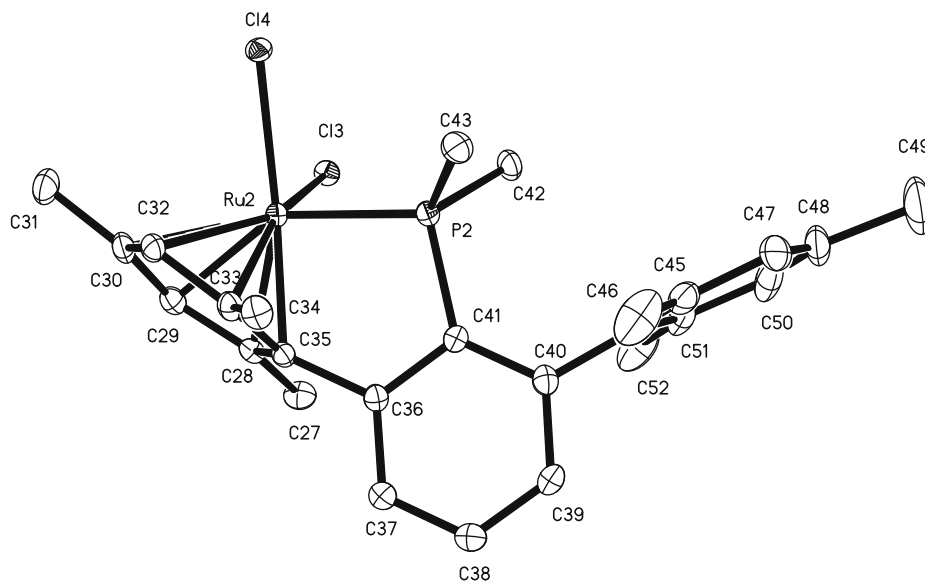


Fig. 8. Molecular structure of **14** (50% ellipsoids). Hydrogen atoms have been omitted for clarity.

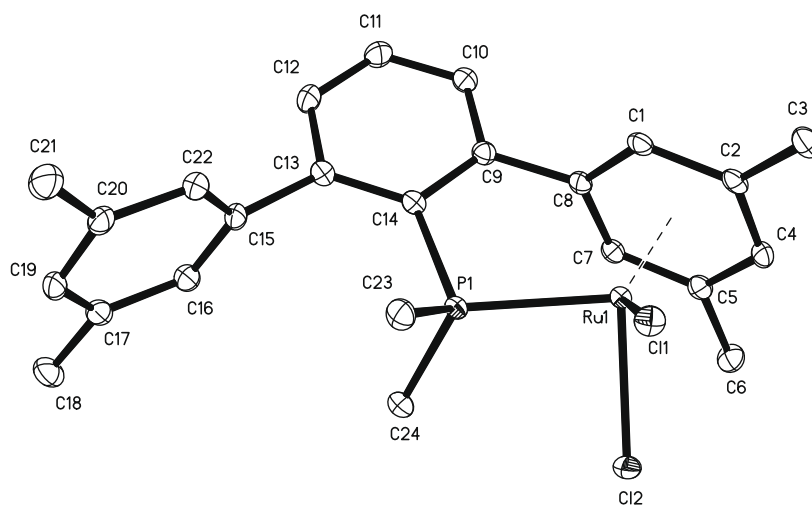


Fig. 9. Molecular structure of **15** (50% ellipsoids). Hydrogen atoms have been omitted for clarity.

the slightly larger phosphine **8** failed to give a complex, and NMR spectra of the reaction mixture showed only the signals of the unreacted starting materials. Refluxing of complexes **11** and **12** and of the reaction mixture of **8** and $\{(p\text{-cymene})\text{RuCl}(\mu\text{-Cl})_2\}$ lead to the elimination of *p*-cymene and intramolecular coordination of one of the flanking arene rings of the *m*-terphenylphosphine ligand. The complexes $\text{Cl}_2\text{RuP}(\text{H}_2)\text{C}_6\text{H}_3\text{-}2\text{-}\eta^6\text{-Mes-6-Mes}$, **13**, $\text{Cl}_2\text{RuP}(\text{Me}_2)\text{C}_6\text{H}_3\text{-}2\text{-}\eta^6\text{-Mes-6-Mes}$, **14**, and $\text{Cl}_2\text{RuP}(\text{Me}_2)\text{C}_6\text{H}_3\text{-}2\text{-}\eta^6\text{-}(3,5\text{-Me}_2\text{C}_6\text{H}_3)\text{-}6\text{-}(3,5\text{-Me}_2\text{C}_6\text{H}_3)$, **15**, were obtained as air-stable red-orange crystalline solids, and the crystal structures of **14** and **15** were determined. There are only a few prior examples of intramolecular arene coordination of biphenyl-2-phosphines to the $[\text{RuCl}_2]$ fragment in the literature [24,25]. For the synthesis of **13** it is important not to exceed a reaction temperature of 70–80 °C in order to avoid unwanted side reactions such as partial elimination of the ligand **6** and concomitant formation of a yet unknown species featuring the phosphide unit $\text{Ru-P}(\text{H})\text{C}_6\text{H}_3\text{-Mes}_2\text{-}2,6$. The exact nature of the high temperature product is not yet known and will be reported in a future contribution. The formation of complexes **13–15** can readily be followed by NMR spectroscopy.

^1H and $^{13}\text{C}\{^1\text{H}\}$ NMR spectra show two sets of signals for the flanking arene rings with the η^6 -coordinated one experiencing a characteristic upfield shift. The ^{31}P NMR resonances display a significant downfield shift of 39.2 ppm (**11–13**) and 32.9 ppm (**12–15**) upon intermolecular arene coordination. The structures of **14** and **15** (Figs. 8 and 9) show that the ruthenium centers lie approximately in the same plain as the central arene rings of the ligands and the phosphorus centers, and that they are positioned almost symmetrically above the coordinated flanking arene rings. The Ru–P distances in **14** and **15** are 2.2991(8) and 2.3181(4) Å and the Ru...C contacts average 2.205(63) and 2.210(63) Å and range from 2.113(2) to 2.287(2) Å and 2.1100(15) to 2.2788(15) Å, respectively. Similar values have been reported for $\text{Cl}_2\text{RuP}(\text{Cy})_2\text{C}_6\text{H}_4\text{-}2\text{-}\eta^6\text{-C}_6\text{H}_4\text{-}2\text{-NMe}_2$: the Ru–P distance is 2.343(2) Å and the Ru...C contacts average 2.200(39) Å [24]. The phosphorus centers in **14** and **15** are bending towards the ruthenium centers as is indicated by the narrow P–C_{ipso}–C_{ortho} angles with values of 113.41(14)° for **14** and 113.66(11)° for **15**. These values are similar to that observed for the free ligand **8**, but differ from **9**. This is due to the fact that with the coordination of phosphorus the *P*-methyl groups of **9**

rotate into the same position above one of the flanking arene rings as in **8** leading to steric repulsion.

4. Summary

A series of *m*-terphenylphosphines TerphPCl₂, TerphPH₂ and TerphPMe₂ was prepared and fully characterized. The structural investigation by X-ray crystallography and density functional theory revealed significant distortions in the environment of the *ipso* carbon and phosphorus centers. These can be traced back to steric interactions and repulsions of the chlorine and methyl substituents on phosphorus with the alkyl groups on the flanking arenes of the *m*-terphenyl substituents. The primary phosphine **6** and the dimethylphosphine **9** readily form complexes with the Cl₂Ru(*p*-cymene) complex fragment. Heating leads to expulsion of the *p*-cymene ligand and intramolecular η⁶ coordination of one of the flanking arene rings to the ruthenium center.

Acknowledgments

Financial Support from the University of Oklahoma, the Florida Institute of Technology, the Petroleum Research Fund administered by the American Chemical Society and the National Science Foundation (CHE-0718446) is gratefully acknowledged. We also thank Prof. J. Clayton Baum at the Florida Institute of Technology for assistance with the quantum chemical calculations.

Appendix A. Supplementary material

Supplementary data associated with this article can be found, in the online version, at doi:10.1016/j.ica.2009.03.034.

References

- [1] L. Weber, Chem. Rev. 92 (1992) 1839–1906.
- [2] M. Yoshifuji, Pure Appl. Chem. 71 (1999) 503–512.
- [3] M. Regitz, O.J. Scherer, Multiple Bonds and Low Coordination in Phosphorus Chemistry, G. Thieme Verlag, Stuttgart, 1990.
- [4] A.F. Littke, G.C. Fu, Angew. Chem., Int. Ed. 41 (2002) 4176–4211.
- [5] D.S. Surry, S.L. Buchwald, Angew. Chem., Int. Ed. 47 (2008) 6338–6361.
- [6] B. Twamley, S.T. Haubrich, P.P. Power, Adv. Organomet. Chem. 44 (1999) 1–65.
- [7] J.A.C. Clyburne, N. McMullen, Coord. Chem. Rev. 210 (2000) 73–99.
- [8] A.A. Diaz, J.D. Young, M.A. Khan, R.J. Wehmschulte, Inorg. Chem. 45 (2006) 5568–5575.
- [9] A.A. Diaz, B. Buster, D. Schomisch, M.A. Khan, J.C. Baum, R.J. Wehmschulte, Inorg. Chem. 47 (2008) 2858–2863.
- [10] R. Riemschneider, B. Diedrich, Ann. 646 (1961) 18–25.
- [11] B. Schiemenz, P.P. Power, Angew. Chem., Int. Ed. Engl. 35 (1996) 2150–2152.
- [12] E. Urnezus, J.D. Protasiewicz, Main Group Chem. 1 (1996) 369–372.
- [13] C. Overländer, J.J. Tirree, M. Nieger, E. Niecke, C. Moser, S. Spirk, R. Pietschnig, Appl. Organomet. Chem. 21 (2007) 46–48.
- [14] R.J. Wehmschulte, M.A. Khan, S.I. Hossain, Inorg. Chem. 40 (2001) 2756–2762.
- [15] A. Saednya, H. Hart, Synthesis (1996) 1455–1458.
- [16] R.S. Simons, S.T. Haubrich, B.V. Mork, M. Niemeyer, P.P. Power, Main Group Chem. 2 (1998) 275–283.
- [17] Bruker AXS, Madison, Wisconsin, 1997.
- [18] R.C. Smith, R.A. Woloszynek, W. Chen, T. Ren, J.D. Protasiewicz, Tetrahedron Lett. 45 (2004) 8327–8330.
- [19] J.C. Tebby (Ed.), CRC Handbook of Phosphorus-31 Nuclear Magnetic Resonance Data, CRC Press, Boca Raton, FL, 1991.
- [20] B. Twamley, C.D. Sofield, M.M. Olmstead, P.P. Power, J. Am. Chem. Soc. 121 (1999) 3357–3367.
- [21] D. Mootz, V. Händler, Z. Anorg. Allg. Chem. 533 (1986) 23–29.
- [22] S. Shah, T. Concolino, A.L. Rheingold, J.D. Protasiewicz, Inorg. Chem. 39 (2000) 3860–3867.
- [23] S.A. Serron, S.P. Nolan, Organometallics 14 (1995) 4611–4616.
- [24] J.W. Faller, D.G. D'Allesi, Organometallics 22 (2003) 2749–2757.
- [25] K. Aikawa, I. Kaito, K. Mikami, Chem. Lett. 36 (2007) 1482–1483.